

# Weierstraß–Institut für Angewandte Analysis und Stochastik

im Forschungsverbund Berlin e.V.

## Simulation of kinetic boundary layers

Hans Babovsky

submitted: 9th February 1995

Weierstrass Institut  
for Applied Analysis  
and Stochastics  
Mohrenstraße 39  
D – 10117 Berlin  
Germany

Preprint No. 140  
Berlin 1995

Edited by  
Weierstraß-Institut für Angewandte Analysis und Stochastik (WIAS)  
Mohrenstraße 39  
D — 10117 Berlin  
Germany

Fax: + 49 30 2004975  
e-mail (X.400): c=de;a=d400;p=iaas-berlin;s=preprint  
e-mail (Internet): preprint@iaas-berlin.d400.de

## Abstract

The numerical transition of a kinetic boundary layer into a steady fluid field via particle simulation is studied. Several modelling aspects are treated. Criteria "measuring" the transition are proposed and studied.

**Keywords:** Kinetic boundary layer, particle simulation, numerical transition.

## 1 Introduction

Kinetic equations on one hand and fluid-dynamic equations on the other hand represent two different levels for the description of large particle systems. The first level - the mesoscopic one - combines detailed features of particle motion, which are free flow and particle collisions; the latter - the macroscopic one - provides some asymptotic limit in which details of the collisions are hidden behind so-called transport coefficients. Kinetic equations are integro-differential equations which describe the evolution of density functions in six-dimensional phase space while the fluid-dynamic description yields moment equations which are a system of partial differential equations in three-dimensional physical space. As a consequence, the numerical solution of gas kinetics requires an amount of computational work which exceeds by far that for fluid-dynamics - if comparable accuracy is desired. Therefore for an efficient numerical code there is a need to combine both descriptions, using fluid-dynamic equations where the macroscopic approach is sufficient and kinetic equations where they are needed.

This problem of coupling different types of equations may be approached at different levels of complexity. In many cases, kinetic effects appear only in thin boundary layers and it may be sufficient to handle these by modelling appropriate slip boundary conditions for fluid-dynamic equations (see, e.g. [17]). In other cases, one has to couple solutions to different types of equations. Such an approach is much more ambiguous, from methodological as well as theoretical points of view. Two central aspects are:

- A full understanding is required of which is the fluid-dynamic counterpart of a given Boltzmann equation and in which sense Navier-Stokes equations reflect the asymptotic behaviour of gas kinetics.
- When coupling Boltzmann solutions with Navier-Stokes solutions, one has to cope with the fact that both types of solutions contain different degrees of information: kinetic solutions provide full information about the distribution in phase space, fluid-dynamic solutions only some moments of this distribution.

Research both on the theoretical side and on the side of numerical experiments is required to end up with a satisfactory numerical scheme for the coupling. Interest in these problems is quite vivid today, due to an increased interest for kinetic equations in applied sciences (for a survey, see [11]). As examples, let us mention on the theoretical side the functional analytic approach in [7, 8] and the stochastic approach in [12]. Focus on numerical aspects is taken in a couple of studies; for a direct numerical coupling of Boltzmann and compressible Navier-Stokes equations see [9, 16]; criteria for a domain

decomposition have been developed in [14]; various aspects - mainly for the coupling of linearized equations - have been studied in [15].

The present paper is a first one in a planned series on numerical experiments concerning the coupling of kinetic and fluid-dynamic equations. A common approach to this field is to develop tools to identify and separate regions which are governed by different types of equations, and to couple solutions by appropriate choice of boundary conditions. An example might be regions in which mean free paths differ by an order of magnitude, so that in one domain the Boltzmann equation has to be solved, while the other one may be safely approximated by the Euler equations. Our view point is slightly different. It relies on the assumption that in certain situations Navier-Stokes equations and the Boltzmann equation provide equivalent first-order corrections to the Euler equations (see [13]). For a coupling of Boltzmann and (compressible) Navier-Stokes solutions, domains have to be identified for which the numerical code for the kinetic equation yields good approximations - not only to *solutions* of the Navier-Stokes equations but also to the *closure relations* which are used to derive the fluid-dynamic equations from the Boltzmann equation. So the focus lies in observing particle simulation solutions and in comparing how situations may generated where these solutions come (in certain domains) as close as possible to the features described by the Navier-Stokes equations. While our intention in the long run is to study more complicated cases, this paper starts with the simplest possible nonlinear situation: the transition of a stationary spatially one-dimensional kinetic boundary layer into a fluid field which is characterized by constant gradients. The numerical kinetic solutions are obtained by Monte Carlo particle simulations as described in [1, 5]. The basic question is: under which circumstances do such schemes (which are not completely well justified as codes for stationary solutions, see [2, 3, 4]) provide the same asymptotic behaviour which are expected for kinetic equations, and what are the corresponding "Navier-Stokes equations". In detail, numerical experiments aim at the following problems:

- to find transition criteria allowing to decide whether a proper transition from kinetics to fluid-dynamics is achieved, and to model such transitions for specific situations,
- to determine the effect of systematic errors of particle simulations for stationary kinetic equations,
- to exploit ways to use simulation schemes for modelling closure relations rather than kinetic solutions, and to use these relations to construct (on a phenomenological level) modified Navier-Stokes equations for the boundary layer.

The paper is organized as follows. In section 2 we discuss the transition from gas kinetics to fluid-dynamics in terms of closure relations and with a result from linearized theory. In section 3 we develop a numerical scheme for the coupling of a one-dimensional boundary layer to a fluid field. Section 4 presents numerical examples and discussions. In three test cases we pick up some of the relevant questions. First, we study a simple relaxation of a boundary layer to a constant fluid field. Second, a thermal layer problem is considered; here, the influence of systematic errors on the heat conduction coefficient

is investigated. Finally, we discuss the modelling of the boundary condition on the fluid dynamics side in an example with a velocity gradient field. Section 5 closes with some conclusions.

## 2 Gas kinetics and fluid dynamics

### 2.1 Boltzmann versus Navier Stokes

The Boltzmann equation is an equation for the density function  $f = f(t, \underline{x}, \underline{v})$  for particles in six-dimensional phase space. (In the following we use the conventions  $\underline{x} = (x, y, z)^T$  and  $\underline{v} = (v_1, v_2, v_3)^T$ .) Its stationary, spatially one-dimensional version reads

$$v_1 \partial_x f(x, \underline{v}) = J(f, f)(x, \underline{v}) \quad (2.1)$$

where  $J(f, f)$  is the Boltzmann collision integral

$$J(f, f)(\underline{v}) = \int_{\mathbb{R}^3} \int_{S^2} k(|\underline{v} - \underline{w}|, \eta) (f(\underline{v}')f(\underline{w}') - f(\underline{v})f(\underline{w})) d^2\eta d^3\underline{w} \quad (2.2)$$

The pair  $(\underline{v}', \underline{w}')$  of "pre-collision velocities" is given by a smooth transformation of the "post-collision velocities"  $(\underline{v}, \underline{w})$  and an "impact parameter"  $\eta$  which is a unit vector in  $\mathbb{R}^3$ . Here we do not need many details about the collision operator and therefore refer the reader to standard literature, e.g. [10]. The only property required is that for any of the five functions  $\phi(\underline{v}) = 1, v_i, |\underline{v}|^2$

$$\int_{\mathbb{R}^3} \phi(\underline{v}) J(f, f)(\underline{v}) d^3\underline{v} = 0 \quad (2.3)$$

Given a density function  $f(\underline{v})$ , define mass and bulk velocities by

$$\rho := \int_{\mathbb{R}^3} f(\underline{v}) d^3\underline{v} \quad (2.4)$$

$$\rho u_i := \int_{\mathbb{R}^3} v_i f(\underline{v}) d^3\underline{v} \text{ for } i = 1, 2, 3 \quad (2.5)$$

internal energy and heat flux vector by

$$\rho e = \frac{1}{2} \int_{\mathbb{R}^3} |\underline{v} - \underline{u}|^2 f(\underline{v}) d^3\underline{v} \quad (2.6)$$

$$q_i = \frac{1}{2} \int_{\mathbb{R}^3} (v_i - u_i) |\underline{v} - \underline{u}|^2 f(\underline{v}) d^3\underline{v} \quad (2.7)$$

and the components of the stress tensor  $P = (p_{ij})_{1 \leq i, j \leq 3}$  by

$$p_{ij} := \int_{\mathbb{R}^3} (v_i - u_i)(v_j - u_j) f(\underline{v}) d^3\underline{v} \quad (2.8)$$

Multiplying the Boltzmann equation with the five abovementioned functions  $\phi$  and integrating yields the five moment equations

$$\partial_x(\rho u_1) = 0 \quad (2.9)$$

$$\partial_x(\rho u_1 \underline{u} + p^{(1)}) = 0 \quad (2.10)$$

$$\partial_x \left( \rho u_1 \left( \frac{1}{2} |\underline{u}|^2 + e \right) + \langle p^{(1)}, \underline{u} \rangle + q_1 \right) = 0 \quad (2.11)$$

where  $p^{(1)} = (p_{11}, p_{12}, p_{13})^T$ . Obviously, one further equation holds:

$$\rho e = \sum_{i=1}^3 p_{ii} =: 3p \quad (2.12)$$

So we have an unclosed system of six equations for the twelve unknowns  $\rho, u_i, p_{ij}, q_1, e$ . This system may be closed by introducing some phenomenological relations expressing  $p_{ij}$  and  $q_1$  in terms of the other quantities. For a Navier-Stokes-Fourier fluid these relations are (see [10, Sections II.8, IV.7]):

$$p_{11} = p - \frac{4\mu}{3} \partial_x u_1 \quad (2.13)$$

$$p_{1i} = -\mu \partial_x u_i \text{ for } i = 2, 3, \text{ and } p_{23} = 0 \quad (2.14)$$

$$p_{22} = p_{33} = p + \frac{2\mu}{3} \partial_x u_1 \quad (2.15)$$

$$q_1 = -\kappa \partial_x e, \text{ and } q_2 = q_3 = 0 \quad (2.16)$$

with viscosity and heat conduction coefficients  $\mu$  and  $\kappa$ . Inserting these yields the following Navier-Stokes equations.

$$\partial_x(\rho u_1) = 0 \quad (2.17)$$

$$\partial_x(\rho(3u_1^2 + e)) = 4\mu \partial_x^2 u_1 \quad (2.18)$$

$$\partial_x(\rho u_1 u_i) = \mu \partial_x^2 u_i \text{ for } i = 2, 3 \quad (2.19)$$

$$\partial_x \left( \rho u_1 \left( \frac{|\underline{u}|^2}{2} + 2e \right) \right) = \kappa \partial_x^2 e + \frac{\mu}{2} \partial_x^2 \left( |\underline{u}|^2 + \frac{1}{3} u_1^2 \right) \quad (2.20)$$

## 2.2 Linearized kinetic boundary layers

There are only few mathematically rigorous results about the transition from a kinetic state to a fluid dynamical state. One of these results concerns linearized equations and is due to Bardos et al. [6]. We shortly comment this situation because it may give some insight for the numerical coupling. For vanishing normal velocity component  $u_1$ , the Navier-Stokes equations reduce to

$$\partial_x(\rho e) = 0, \quad (2.21)$$

$$\partial_x^2 u_i = 0, \quad i \neq 1 \quad (2.22)$$

and

$$\partial_x^2 \left( \kappa e + \frac{\mu}{2}(u_2^2 + u_3^2) \right) = 0. \quad (2.23)$$

Linearization around some constant state  $(\hat{\rho}, \hat{u}_2, \hat{e})$ , ( $u_3 \equiv 0$  for simplicity) replaces (2.21) and (2.23) with

$$\partial_x \left( \frac{\rho}{\hat{\rho}} + \frac{e}{\hat{e}} \right) = 0 \quad (2.24)$$

and

$$\partial_x^2 e = 0. \quad (2.25)$$

The solution is given by the linear profiles

$$u_2 = u_0 + u^{(\infty)} x \quad (2.26)$$

$$e = e_0 + e^{(\infty)} x \quad (2.27)$$

and

$$\rho = \rho_0 - \frac{\hat{\rho}}{\hat{e}} x \quad (2.28)$$

As Bardos et al. showed, there is a smooth transition of kinetic boundary layers (based on the linearized Boltzmann equation) to such linear profiles. More precisely, they prove the following. Given any number  $m_f \in \mathbb{R}$  (the mass flux through the plane  $x = \text{const}$ ), any integrable inflow distribution  $\phi$  at  $x = 0$ , and numbers  $u_\infty, e_\infty$  there exists a unique solution (in a certain weighted  $L^2$  space) of the linearized Boltzmann equation

$$v_1 \partial_x f = Lf \quad (2.29)$$

with inflow condition at  $x = 0$

$$f(x, v) = \phi(v) \text{ for } v_1 > 0 \quad (2.30)$$

with mass flux

$$\int_{\mathbb{R}^3} v_1 f(x, v) d^3 v = m_f \quad (2.31)$$

and with the asymptotic behaviour

$$\lim_{x \rightarrow \infty} \frac{d}{dx} \int_{\mathbb{R}^3} v_2 f d^3 v = u_\infty \quad (2.32)$$

$$\lim_{x \rightarrow \infty} \frac{d}{dx} \frac{1}{3} \int_{\mathbb{R}^3} (v^2 - 3) f d^3 v = e_\infty \quad (2.33)$$

Here  $L$  is the collision operator linearized around the Maxwellian  $M(v) = (2\pi)^{-3/2} \exp(-v^2/2)$ :

$$Lf(v) = \int_w \int_\eta k(\cdot, \cdot) (M(v')f(w') + M(w')f(v') - M(v)f(w) - M(w)f(v)) d\eta dw \quad (2.34)$$

Moreover, from these results follows that  $f$  can be decomposed into three parts:  $f = F + G + H$ , where

- $F$  is the so-called hydrodynamic part:

$$F(x, v) = x \left( u_\infty v_2 + \frac{1}{2} e_\infty (|v|^2 - 5) \right) M(v) \quad (2.35)$$

- $G$  is  $x$ -independent and the unique solution orthogonal (with a suitable scalar product) to the null space of  $L$  of

$$v_1 \partial_x F = LG \quad (2.36)$$

(This solution does not contribute to the macroscopic variables and is also called the fluctuation part)

- $H$  is the boundary layer solution (solution to Milne problem):

$$v_1 H = LH, \quad H(0, v) = \phi(v) - G(v) \text{ for } v_1 > 0 \quad (2.37)$$

which for  $x \rightarrow \infty$  converges exponentially fast to a function

$$H_\infty = (a_\infty + m_f v_1 + b_\infty v_2 + c_\infty v^2) M \quad (2.38)$$

**Remarks:** Consider linearized boundary layers for given gradients  $u_\infty, e_\infty \in \mathbb{R}$ , for  $m_f = 0$  and for given inflow condition  $\phi$ .

1. *Slip conditions:* The slip conditions necessary to match the linear profiles to the kinetic boundary layers are obtained from  $a_\infty, b_\infty$  and  $c_\infty$  (which in general are not known in advance).

2. *Scaling:*  $G = u_\infty G_1 + e_\infty G_2$  where  $G_1$  and  $G_2$  are the unique solutions of  $v_1 v_2 M = LG_1$  and  $\frac{1}{2}v_1(v^2 - 5)M = LG_2$ ; furthermore,  $H = H_0 - u_\infty H_1 - e_\infty H_2$  where  $H_i$  are solutions of  $v_1 H = LH$  with inflow conditions given by  $\phi$ ,  $G_1$  and  $G_2$ .
3. *Fluid dynamic limit:* Consider the boundary layer described by  $v_1 \partial_x f = \epsilon^{-1} J(f)$ , with prescribed gradients  $u_\infty$  and  $e_\infty$  for the fluid field close to the boundary. A change of variables  $\xi := \epsilon^{-1} x$  changes the kinetic equation into  $v_1 \partial_\xi f = J(f)$  and the gradients into  $\epsilon u_\infty$  and  $\epsilon e_\infty$ . Thus the corresponding linearized correction terms are  $G = \epsilon(u_\infty G_1 + e_\infty G_2)$  and  $H = H_0 + \epsilon(u_\infty H_1 + e_\infty H_2)$ . In the limit  $\epsilon \rightarrow 0$ , the remaining slip condition is that belonging to the solution  $H_0$  of the Milne problem.  $H_0$  vanishes for thermalized inflow conditions, i.e. for  $\phi = M$ .

## 3 Numerical coupling

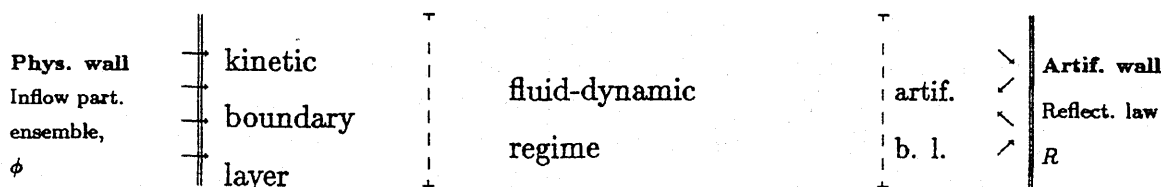
### 3.1 Design of an algorithm

Our aim is to design an algorithm which allows for the numerical transition from the kinetic boundary layer to the fluid-dynamic regime. At first sight, the most natural idea seems to run a simulation scheme on an interval with kinetic boundary conditions on one side and with fluid-dynamic boundary conditions on the other side. We are facing the following difficulties.

- While it is natural to assume the kinetic inflow condition to be known, the fluid-dynamic one is not. Look at the linearized case of section 2.2. There the asymptotic behaviour of the layer is known only up to a few constants. We should not expect more in the nonlinear case. Moreover, the solutions of the linearized case are partially "unphysical" in the sense that they may assume negative values. Therefore we are far from knowing the details of the velocity distribution in the fluid-dynamic regime.
- The method of time-averaging to obtain stationary solutions is affected with a systematic error [2, 3]. So we have to investigate carefully whether such an error comes into play in our case.

For the numerical procedure, we apply the simulation scheme described in [1, 5] to a large ensemble of particles: alternately the particles are exposed to a shift phase (where the positions are changed due to particle velocities:  $x(i) \rightarrow x(i) + \Delta t v_x(i)$ ), and to a collision step (where particles are collected into pairs  $(i, n(i))$  which perform random velocity changes  $(v(i), v(n(i))) \rightarrow (v'(i), v'(n(i)))$ ). We use the version for which energy and momenta are strictly conserved (see [1, section 7]). For the collision step, physical (one-dimensional) space is divided into cells; only particles occupying the same cell may form a pair. These steps are applied many times; the macroscopic variables of interest are obtained during the run via time-averaging.

**Fig.1: The computational domains**



Three domains are intended to be generated by running the algorithm. A physical boundary layer domain at one side of the physical domain, an artificial boundary layer on the other side, and a fluid-dynamic regime in between. This situation is demonstrated in Fig. 1. In the region behind the physical wall, a reservoir of particles is generated with a velocity distribution according to the inflow condition for the kinetic layer. During the shift phase, a part of these particles enters the physical domain thus generating the correct boundary condition. At the artificial layer, a reflection boundary condition is applied. The reflection law - depending if necessary on a few parameters to be matched - is intended to generate an inflow as close as possible to the correct fluid-dynamic flow in order to make the artificial boundary layer as narrow as possible. Let us have a short look again to the linearized case. The results of section 2.2 may be interpreted as follows. Given constants  $m_f, u_\infty, e_\infty$ , there exists a unique mapping from the infinite-dimensional function space of inflow conditions to the parameters  $a_\infty, b_\infty, c_\infty$ . Necessary for the matching of two kinetic layers "from the left" and "from the right" with a fluid-dynamic zone in between seems to be that the corresponding parameters are compatible. Whenever necessary, we try to achieve this by matching a few parameters in the reflection law for the artificial layer. (We leave uncommented the possible role of the fluctuation part in this context.)

### 3.2 Coupling conditions, transition criteria

The difference between the moment equations for the Boltzmann equation and the Navier-Stokes equations lies in the phenomenological relations (2.13) to (2.16). Therefore, we use these as the key for the transition from the kinetic regime to the fluid dynamic regime. They allow to formulate (although only necessary) conditions whether in a distance to the wall the fluid-dynamic description is appropriate or such a state is not reached (maybe through an inappropriate choice of the reflection law at the artificial boundary). Aspects concerning the correct handling are illustrated in the following two examples.

- In the absence of velocity gradients, the closure relations for the pressure coefficients read

$$p_{11} = p_{22} = p_{33} = p \quad (3.1)$$

$$p_{ij} = 0 \text{ for } i \neq j \quad (3.2)$$

Under these conditions, the equations  $\partial_x p^{(1)} = 0$  (from the Boltzmann equation) and  $\partial_x(\rho e) = 0$  (Navier-Stokes) are equivalent. Therefore reasonable necessary criteria are  $3p_{ii}/(p_{11} + p_{22} + p_{33}) = 1$  for  $i = 2, 3$ , and  $p_{ij} = 0$  for  $i \neq j$ .

- One of the closure relations claims that the heat flow depends linearly (through the heat coefficient) on the temperature gradient. It is important to control this quantity in order to obtain a coupling to the correct Navier-Stokes equations. Viscosity coefficients depend sensitively on the collision rate in a gas. As was shown in [3], a necessary criterion to construct a reliable simulation scheme for stationary solutions is to efficiently control the collision frequency. In the next subsection we describe one method applicable in our simple case. In the section about numerical experiments we test its effect.

A numerical experiment for a model Boltzmann equation with two-dimensional velocity space (for details see section 4.1) demonstrates the importance of an appropriate choice of the reflection law at the artificial boundary. Let us consider the relaxation of a boundary layer into a constant fluid field with zero velocities. The inflow condition is chosen different from a Maxwellian thus generating a boundary layer. Linear theory (which we consult because of the lack of comparable results in nonlinear theory) prescribes at the right hand side a function of the form  $(1 + a_\infty + c_\infty v^2)M$ . Reflection laws compatible with such functions are for example specular reflection or (because of spherical symmetry) the reflection law changing  $\underline{v}$  into  $|\underline{v}|(-\cos \alpha, \sin \alpha)^T$ ,  $\alpha \in [-\pi/2, \pi/2]$ , with an angular distribution proportional to  $|\cos \alpha|$  (BC1). Not compatible is an angular equidistribution in an interval  $[-\pi/2 + \epsilon, \pi/2 - \epsilon]$  with  $\epsilon > 0$  small (BC2). Fig.2 compares  $p_{corr} := 2p_{ii}/(p_{11} + p_{22})$  (solid line for  $i = 1$ ) indicating a fluid-dynamic region on the right part of the interval for (BC1) but no such region for (BC2).

### 3.3 Control of collision frequencies

In [2] we investigated time averaged simulations as numerical schemes to construct steady solutions of the Boltzmann equation. As expected, it turned out that this approach is affected with a systematic error which is due to the nonlinearity of the collision operator. An explicit formula shows the connection of this error with covariances of the occupation numbers of the generated particle ensemble. In [3] we formulated sufficient conditions for an abstract scheme in order to get rid of this deficiency. Three conditions appeared to be crucial. Besides the existence of a stationary measure for the generated Markov process these were ergodicity and a certain factorization property of the local particle distribution. One of the implications of these investigations was that simulation

schemes as that described above lead to collision frequencies which are larger than those required from theory. (For a quick argument on this, see [4].)

Fig.2a: Correction factors for pressure matrix, BC1

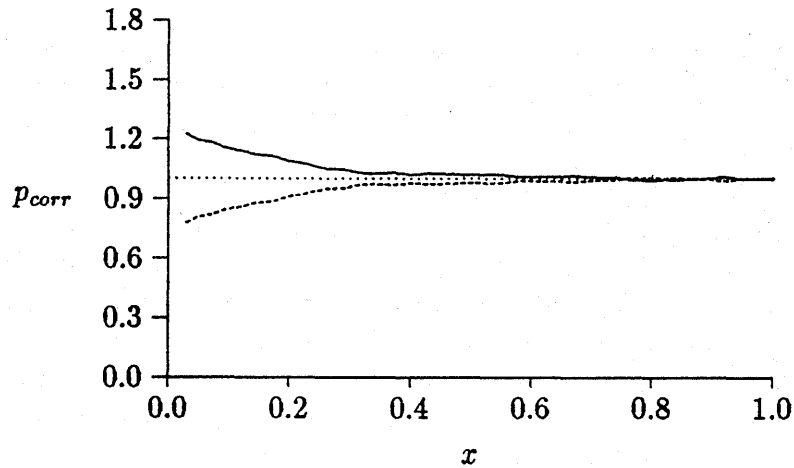
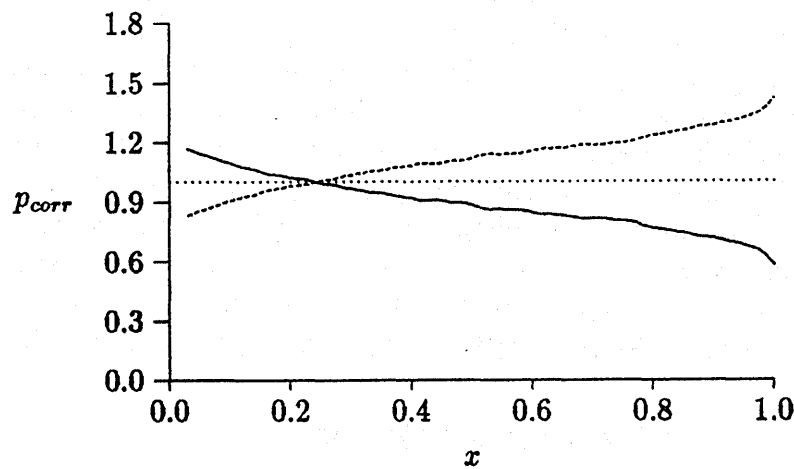


Fig.2b: Correction factors for pressure matrix; BC2



Wrong collision frequencies may result in particular in wrong viscosity and heat conduction coefficients. Therefore a means to measure such artificial effects may be to measure the deviation of these coefficients from the correct ones. Therefore we build up an alternative scheme for which the mean number of collisions is better controlled. For this scheme, the steady Boltzmann equation is modified into an equivalent version. Start with the Boltzmann equation of section 2.1. Introducing a transformation  $\xi(x)$  of

the spatial variable transforms the Boltzmann equation into

$$v_1 \partial_\xi f(\xi, \underline{v}) = \frac{1}{\partial_x \xi} J(f, f)(\xi, \underline{v}) =: \tilde{J}(f, f)(\xi, \underline{v}) \quad (3.3)$$

If the collision kernel  $k(., .)$  is independent of the velocities (in particular if it is constant) then the choice of  $\partial_x \xi := c\rho(x)$  leads to a loss term for  $\tilde{J}(f, f)$  which is equal to  $f(\xi, \underline{v})$  and thus represents constant collision probabilities. These can obviously be reproduced correctly in a simulation. A short inspection of the convergence proofs in [1, 5] shows that a modified simulation scheme with constant collision probabilities produces convergent approximations of the evolution problem

$$(\partial_t + v_1 \partial_\xi) f = \tilde{J}(f, f) \quad (3.4)$$

The steady solutions of this problem may be readily transformed back into solutions of the original problem.

We would like to stress that results generated with this alternative do not appear to be as stable as with the code described before. Therefore it is not as useful for production runs. Our main aim was to find some means to estimate artificial effects resulting from perturbed collision numbers. As is demonstrated in the next section, there is a clear trend when passing from one code to another. Therefore for us these results seem to be of relevance.

## 4 Numerical results

### 4.1 The setting

This is a study on fundamental questions about numerical simulations rather than on particular physical results. Therefore we search for a situation where perturbations caused by random effects are small - even for modest particle numbers. This is the reason why we consider here exclusively the case of a two-dimensional velocity domain. However, there is no reason for any doubts about the immediate relevance of the results for the three-dimensional case.

The Boltzmann equation under investigation is given by the collision integral

$$J(f, f)(\underline{v}) = \frac{1}{\pi} \int_{\mathbb{R}^2} \int_0^\pi (f(\underline{v}') f(\underline{w}') - f(\underline{v}) f(\underline{w})) d\alpha d^2 \underline{w} \quad (4.1)$$

where  $\underline{v}' = \underline{v} - \eta < \underline{v} - \underline{w}, \eta >$ ,  $\underline{v}' + \underline{w}' = \underline{v} + \underline{w}$  and  $\eta = (\cos \alpha, \sin \alpha)^T$ . As inflow conditions we choose in all cases linear combinations of the form

$$f_0(\underline{v}) = (1 - \lambda_{in}) M_{1,0,1}(\underline{v}) + \lambda_{in} \delta_{(1,0)}(\underline{v}) \quad (4.2)$$

where  $M_{\rho,u,T}$  denotes the Maxwellian (in  $\mathbb{R}^2$ ) with density  $\rho$ , bulk velocities  $u_1 = 0$ ,  $u_2 = u$  and temperature  $T$ , and  $\delta_{(1,0)}$  is the delta function concentrated on the velocity  $\underline{v} = (1, 0)$ . The reflection laws on the right hand side are (except in section 4.4) given

by the angular distribution of (BC1) in section 3.2 and - if a temperature gradient is to be generated - by an increase of the modulus of the velocity  $|\underline{v}| \rightarrow c|\underline{v}|$ . The use of non-absorbing reflection laws guarantees zero mass flux in all cases.

The spatial domain  $[0, 1]$  is divided into 100 intervals of equal length. In each cell, the homogeneous spatial density  $\rho \equiv 1$  is represented by 24 particles. The simulation starts with uniform distribution over all cells. As a preprocessing step, as many simulation time steps are performed as are needed to end up in a quasi-steady state. For the evaluation, time averages over 1000 time steps are calculated.

## 4.2 The boundary layer problem

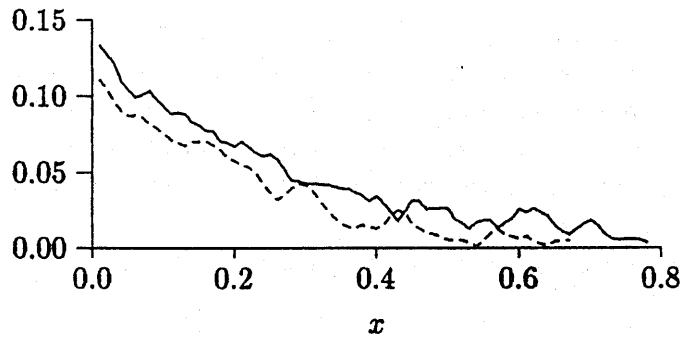
As a first test case we study the pure boundary layer problem with zero bulk velocities and zero gradients at  $x \rightarrow \infty$ . The moment equations for the Boltzmann equation reduce to

$$\partial_x p_{11} = \partial_x p_{12} = 0 \quad (4.3)$$

$$\partial_x q_1 = 0 \quad (4.4)$$

Since we use symmetric inflow conditions on the left and an energy preserving symmetric reflection law on the right hand side, the solution is given by  $p_{11} = \text{const}$ ,  $p_{12} = 0$  and  $q_1 = 0$ .

Fig.3: Pressure and temperature corrections



The corresponding Navier-Stokes equations are

$$\partial_x(p_{11} + p_{22}) = 0 \quad (4.5)$$

$$\partial_x^2 e = 0 \quad (4.6)$$

with the solution  $p_{11} = p_{22} = \text{const}$ ,  $e = \text{const}$ . Notice that  $p_{11} = p_{22}$  has been assumed when deriving the Navier-Stokes equations. Under this assumption, the first Boltzmann

moment equation and the first Navier-Stokes equation coincide. Therefore this condition may well be used as a (necessary) criterion to distinguish between the kinetic and the fluid dynamic regime.

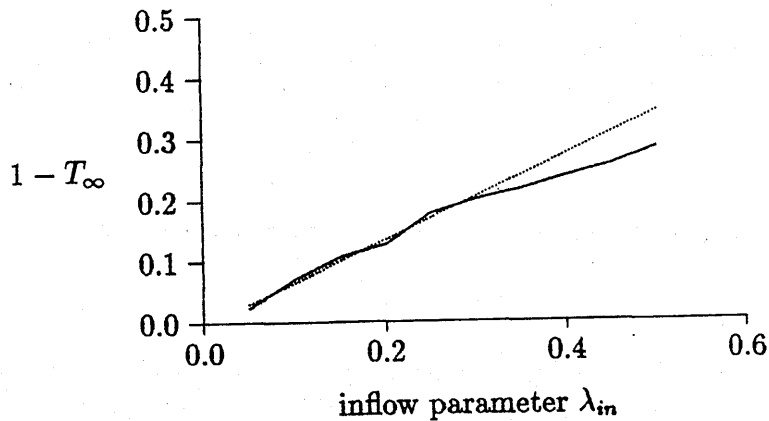
For our test cases, we use the inflow conditions (4.2) For the associated Milne problem we obtain

$$f = M + \lambda_{in} H \quad (4.7)$$

i.e. a perturbation of the Maxwellian depending linearly on  $\lambda_{in}$ . As Fig. 2a demonstrates for a typical situation,  $p_{corr} := 2p_{ii}/(p_{11} + p_{22})$  assumes values close to 1 only in a region sufficiently far away from the left boundary layer. (A kinetic layer close to the artificial boundary cannot be identified.) In the boundary region the closure relations have to be modified into  $p_{11} =: p = p_{22} + \Delta p_{22}$  with some correction function  $\Delta p_{22} = \Delta p_{22}[\lambda_{in}]$ .  $\Delta p_{22}$  which relaxes to 0 for large  $x$  is shown in Fig. 3 (solid line). It may reasonably well be approximated by an exponential. Similarly the equation relating heat flux and temperature gradient has to be modified. While the heat flux is identically zero, the temperature relaxes to a constant value  $T_\infty$  for  $x$  large:  $T(x) = T_\infty + \Delta T(x)$ .  $\Delta T$  (which again is a function of  $\lambda_{in}$ ) is shown in Fig. 3 (dotted line); both lines in Fig. 3 refer to  $\lambda_{in} = 0.25$ . The modified closure relation reads  $q_1 = 0 = -\kappa \partial_x (T - \Delta T)$ .

Linearized theory claims a linear dependence of the temperature jump  $1 - T_\infty$  on the inflow parameter  $\lambda_{in}$ . As Fig. 4 demonstrates, the simulation scheme reflects this relation reasonably well for  $\lambda_{in}$  small enough.

Fig.4: Temperature jump



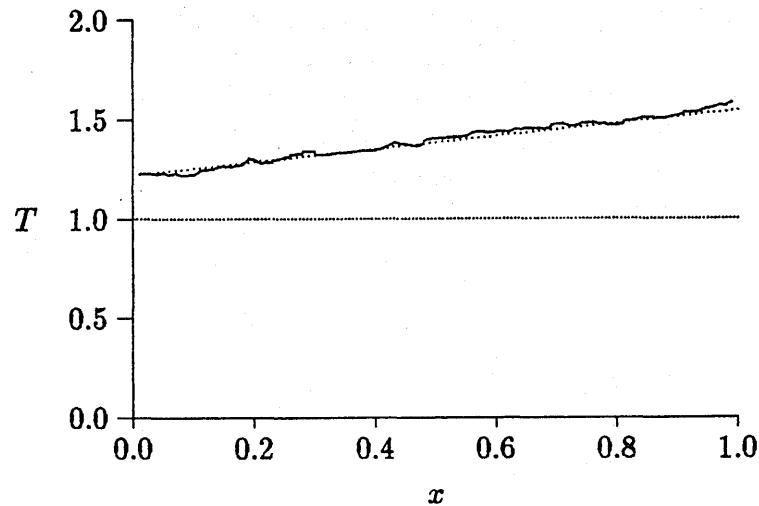
### 4.3 The thermal layer problem

We investigate the coupling of a boundary layer to a field with zero bulk velocities and constant non-zero temperature gradient. As inflow condition we choose the Maxwellian

with temperature 1. At least linear theory then predicts that no boundary layer appears here. The reflection law at the right hand side is that of the previous example, but the modulus of the velocity is increased by a fixed factor.

The relevant Boltzmann moment equations and Navier-Stokes equations are the same as before. Fig. 5 shows a typical temperature profile which comes out of the simulation run. As expected, no boundary layers appear, and the temperature is very well approximated by a linear profile. In this test example it is instructive to compare the results with the prediction from linearized theory, and to investigate the effective heat conduction coefficient. The latter depends sensitively on the collision rate. Therefore a comparison between the standard algorithm ("version 1") and the alternative described in section 3.3 ("version 2") might be of interest.

Fig.5: Temperature (solid), lin. approx. (dotted)



Linearized theory as exposed in section 2.2 predicts a temperature profile of the form

$$T(x) = 1 + a + bx \quad (4.8)$$

with a fixed ratio  $\lambda = a/b = a/\partial_x T$ . We ran several test runs with different temperature gradients in order to test the hypothesis of a fixed  $\lambda$ . Fig. 6a (solid line) shows  $a = a(\partial_x T)$  for version 1 and indicates that linear dependence is indeed very well satisfied. However, there is a difference between version 1 and version 2 (Fig.6a; dotted lines represent the linear approximations). We find out that  $\lambda_2$  is increased compared to  $\lambda_1$  by a factor of 1.26.

Denote by  $T_{av}$  the average temperature in the slab. From the above it follows that  $T_{av} = 1 + a + 0.5 * b$  and  $T_{av} - 1 = (0.5 + \lambda_i) * \partial_x T$ . In particular,  $T_{av} - 1$  is a measure for the temperature gradient. In Fig. 6b the heat flux is plotted versus  $T_{av}$ . It turns out that the assumption of a linear dependence is well satisfied for small temperature

gradients. There the curves for version 1 and 2 coincide. For larger values the heat flux grows faster than the linear profile. For the heat coefficient  $\kappa = q_1/\partial_x T$  we find a value for version 1 which is decreased by a factor  $(\lambda_1 + 0.5)/(\lambda_2 + 0.5) \approx 0.87$  as compared to version 2.

Fig.6a: Temperature jump versus temperature gradient

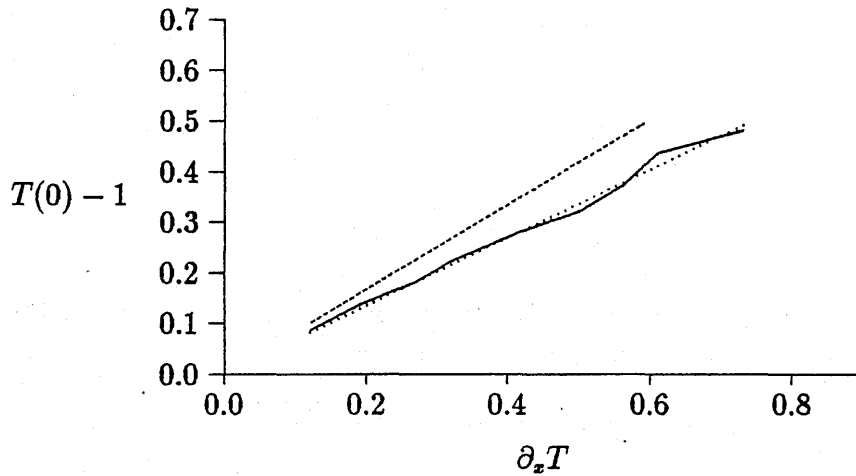
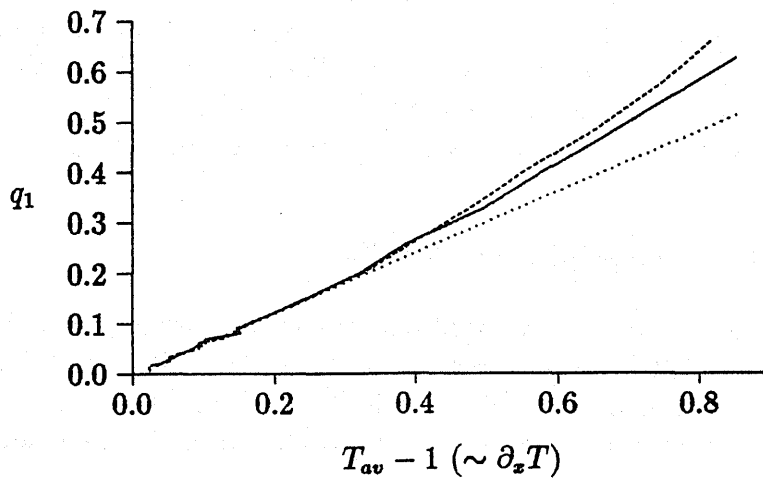


Fig.6b: Heat flow versus temperature gradient



## 4.4 Velocity jump conditions

As a last example, we consider the matching to a tangential velocity field  $u_2 \neq 0$ . Under the condition  $u_1 = 0$ , the Boltzmann moment equations become

$$\partial_x p_{11} = 0, \quad \partial_x p_{12} = 0 \quad (4.9)$$

$$\partial_x (p_{12} u_2 + q_1) = 0 \quad (4.10)$$

and the Navier-Stokes equations are

$$\partial_x (\rho e) = 0 \quad (4.11)$$

$$\partial_x^2 u_2 = 0 \quad (4.12)$$

$$\partial_x^2 \left( \kappa e + \frac{\mu}{2} u_2^2 \right) = 0 \quad (4.13)$$

In this situation it is not clear in advance how to model the reflection law on the fluid side. We performed numerical experiments with the ansatz

$$\underline{v}' := (1 - r) |\underline{v}| (\cos \alpha, \delta \sin \alpha + \sqrt{1 - \delta^2})^T \quad (4.14)$$

(version 1) and with

$$\underline{v}' := |\underline{v}| ((1 - r_1) \cos \alpha, (1 - r_2) \sin \alpha)^T + (0, r_3)^T \quad (4.15)$$

(version 2), with an angular distribution as in (BC1). In version 1, we found that the closure relations can reasonably be achieved only in a small range for the ratio  $r/\delta$ . More stable results were obtained with version 2. (We used fixed ratios  $r_2/r_1 = 1.5$  and  $r_3/r_1 = 1.75$ .) Figures 7 show the velocity gradient and the pressure coefficient  $p_{12}$  for version 2 for different  $\lambda_{ref} = 5r_1$ . The dotted line (version 2) and the dashed line (version 1) show the best linear approximations (for  $\lambda_{ref}$  small). They indicate that the viscosity coefficient depends (at least slightly) on the reflection model.

## 5 Some concluding remarks

The Boltzmann equation and the Navier-Stokes equations are expected to provide in some asymptotic sense equivalent descriptions of a fluid flow. The studies of this paper were motivated by the hope that the situation is similar for particle simulation schemes and that these may be used for a proper numerical coupling of gas kinetic and fluid-dynamic solutions.

It turned out that such a behaviour is really reflected in simulation runs. However, for a proper coupling of different regimes, a couple of modelling aspects have to be considered. First, stable, well-defined transport coefficients come out only in situations of

modest gradients. (That's what one might expect from theory.) Second, much depends on the modelling of the artificial boundary. Different choices of reflection laws give rise to different macroscopic behaviour and with this to different Navier-Stokes equations.

As efficient criteria for the observation of the transition turned out the closure relations, in particular the pressure coefficients and the transport coefficients. These may be easily controlled during a simulation run, and if they are satisfied, gas kinetic and fluid-dynamic description are equivalent.

Fig.7a: Velocity gradient

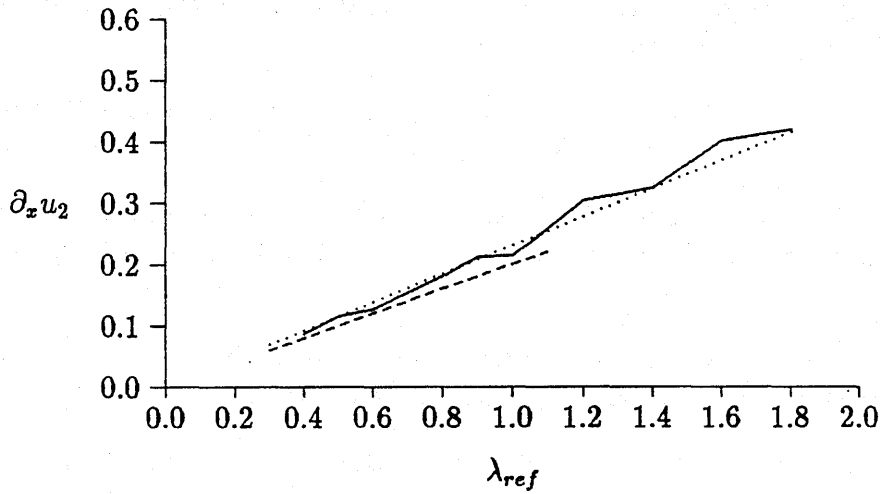
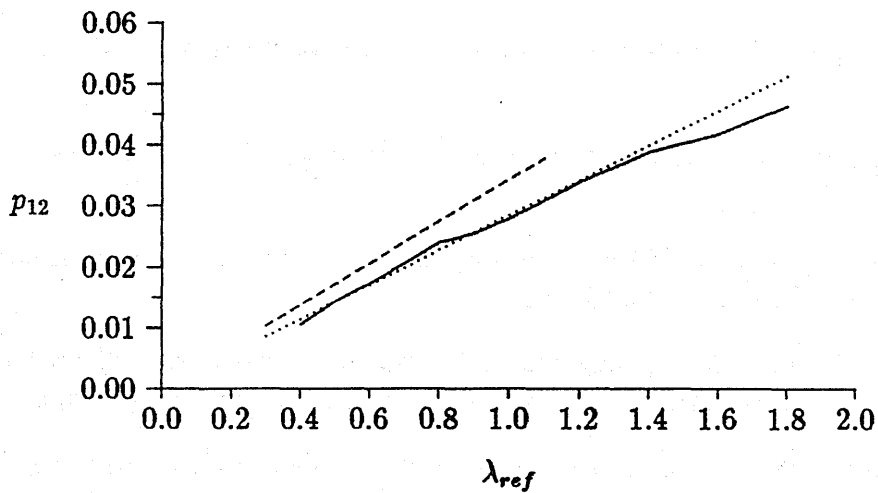


Fig.7b: Pressure coefficient  $p_{12}$



## References

- [1] H. Babovsky. A convergence proof for Nanbu's Boltzmann simulation scheme. *European J. Mech., B/Fluids*, 8:41–55, 1989.
- [2] H. Babovsky. Time averages of simulation schemes as approximations to stationary kinetic equations. *Eur. J. Mech., B/Fluids*, 11:199–212, 1992
- [3] H. Babovsky. Monte Carlo simulation schemes for steady kinetic equations. *Transp. Theory Stat. Phys.*, 23:249–264, 1994.
- [4] H. Babovsky. Systematic errors in stationary Boltzmann simulation schemes. In: *Rarefied Gas Dynamics: Theory and Simulations*, B. Shizgal, D. Weaver (eds.), AIAA, Washington 1994, pp.174–182.
- [5] H. Babovsky and R. Illner. A Convergence proof for Nanbu's simulation method for the full Boltzmann equation. *SIAM J. Numer. Anal.*, 26:45–65, 1989.
- [6] C. Bardos, R. Caflisch, and B. Nicolaenko. The Milne and Kramers problems for the Boltzmann equation of a hard sphere gas. *Comm. Pure Appl. Math.*, 39:323–352, 1986.
- [7] C. Bardos, F. Golse, and D. Levermore. Fluid dynamic limits of kinetic equations I. Formal derivations. *J. Statist. Phys.*, 63:323–344, 1991.
- [8] C. Bardos, F. Golse, and D. Levermore. Fluid dynamic limits of kinetic equations II. Convergence proofs for the Boltzmann equation. *Comm. Pure Appl. Math.*, 46:667–753, 1993.
- [9] J.-F. Bourgat, P. Le Tallec, D. Tidriri, and Y. Qiu. *Numerical coupling of nonconservative or kinetic models with the conservative compressible Navier-Stokes equations*. INRIA preprint 1426, 1991.
- [10] C. Cercignani. *The Boltzmann equation and its applications*. Springer, New York, 1988.
- [11] C. Cercignani. Mathematical models in rarefied gas dynamics. *Surv. Math. Ind.*, 1:119–143, 1991.
- [12] C. Costantini and R. Marra. Hydrodynamic Limits for the Boltzmann Process. *Journ. Stat. Phys.*, 67:229–249, 1992.
- [13] H. Grad. Asymptotic equivalence of the Navier-Stokes and nonlinear Boltzmann equations. In: *Symposia in Applied Math.*, 17, Amer. Math. Soc., 1965.
- [14] F. Gropengießer. *Gebietszerlegung bei Strömungen im Übergangsbereich zwischen Kinetischer Theorie und Aerodynamik*. PhD thesis, University of Kaiserslautern, 1991.

- [15] A. Klar. *Domain decomposition for kinetic and aerodynamik equations*. PhD thesis, University of Kaiserslautern, 1994.
- [16] A. Lukschin, H. Neunzert, J. Struckmeier. *Coupling of Navier-Stokes and Boltzmann regions*. Interim Report for the HERMES project DPH 6473/91, 1992.
- [17] P. Rostand. Kinetic boundary layers, numerical simulations. *Journ. Comp. Phys.*, 86:18–55, 1990.

## Recent publications of the Weierstraß-Institut für Angewandte Analysis und Stochastik

### Preprints 1994

111. Vladimir Maz'ya, Gunther Schmidt: On approximate approximations using Gaussian kernels.
112. Henri Schurz: A note on pathwise approximation of stationary Ornstein-Uhlenbeck processes with diagonalizable drift.
113. Peter Mathé: On the existence of unbiased Monte Carlo estimators.
114. Kathrin Bühning: A quadrature method for the hypersingular integral equation on an interval.
115. Gerhard Häckl, Klaus R. Schneider: Controllability near Takens-Bogdanov points.
116. Tatjana A. Averina, Sergey S. Artemiev, Henri Schurz: Simulation of stochastic auto-oscillating systems through variable stepsize algorithms with small noise.
117. Joachim Förste: Zum Einfluß der Wärmeleitung und der Ladungsträgerdiffusion auf das Verhalten eines Halbleiterlasers.
118. Herbert Gajewski, Konrad Gröger: Reaction-diffusion processes of electrically charged species.
119. Johannes Elschner, Siegfried Prössdorf, Ian H. Sloan: The qualocation method for Symm's integral equation on a polygon.
120. Sergej Rjasanow, Wolfgang Wagner: A stochastic weighted particle method for the Boltzmann equation.
121. Ion G. Grama: On moderate deviations for martingales.
122. Klaus Fleischmann, Andreas Greven: Time-space analysis of the cluster-formation in interacting diffusions.
123. Grigori N. Milstein, Michael V. Tret'yakov: Weak approximation for stochastic differential equations with small noises.
124. Günter Albinus: Nonlinear Galerkin methods for evolution equations with Lipschitz continuous strongly monotone operators.

125. Andreas Rathsfield: Error estimates and extrapolation for the numerical solution of Mellin convolution equations.
126. Mikhail S. Ermakov: On lower bounds of the moderate and Cramer type large deviation probabilities in statistical inference.
127. Pierluigi Colli, Jürgen Sprekels: Stefan problems and the Penrose–Fife phase field model.
128. Mikhail S. Ermakov: On asymptotic minimaxity of Kolmogorov and omega-square tests.
129. Gunther Schmidt, Boris N. Khoromskij: Boundary integral equations for the biharmonic Dirichlet problem on nonsmooth domains.
130. Hans Babovsky: An inverse model problem in kinetic theory.
131. Dietmar Hömberg: Irreversible phase transitions in steel.
132. Hans Günter Bothe: How 1-dimensional hyperbolic attractors determine their basins.
133. Ingo Bremer: Waveform iteration and one-sided Lipschitz conditions.
134. Herbert Gajewski, Klaus Zacharias: A mathematical model of emulsion polymerization.
135. J. Theodore Cox, Klaus Fleischmann, Andreas Greven: Comparison of interacting diffusions and an application to their ergodic theory.
136. Andreas Juhl: Secondary Euler characteristics of locally symmetric spaces. Results and Conjectures.
137. Nikolai N. Nefedov, Klaus R. Schneider, Andreas Schuppert: Jumping behavior in singularly perturbed systems modelling bimolecular reactions.
138. Roger Tribe, Wolfgang Wagner: Asymptotic properties of stochastic particle systems with Boltzmann type interaction.

### Preprints 1995

139. Werner Horn, Jan Sokolowski, Jürgen Sprekels: Control problems with state constraints for the Penrose–Fife phase-field model.